Shiga Toxin 1-Induced Proinflammatory Cytokine Production Is Regulated by the Phosphatidylinositol 3-Kinase/Akt/Mammalian Target of Rapamycin Signaling Pathway[▽]

Rama P. Cherla, Sang-Yun Lee, Renée A. Mulder, Moo-Seung Lee, and Vernon L. Tesh*

Department of Microbial and Molecular Pathogenesis, College of Medicine, Texas A&M University System Health Science Center, College Station, Texas 77843-1114

Shiga toxin 1 (Stx1) transiently increases the expression of proinflammatory cytokines by macrophage-like THP-1 cells in vitro. Increased cytokine production is partly due to activation of the translation initiation factor eIF4E through a mitogen-activated protein kinase (MAPK)- and Mnk1-dependent pathway. eIF4E availability for translation initiation is regulated by association with eIF4E binding proteins (4E-BP). In this study, we showed that Stx1 transiently induced 4E-BP hyperphosphorylation, which may release eIF4E for translation initiation. Phosphorylation of 4E-BP at priming sites T37 and T46 was not altered by Stx1 but was transiently increased at S65, concomitant with increased cytokine expression. Using kinase inhibitors, we showed that 4E-BP phosphorylation was dependent on phosphatidylinositol 3-kinase (PI3K), Akt, and mammalian target of rapamycin (mTOR) activation but did not require MAPKs. Stx1 treatment resulted in increased levels of cytosolic Ca^{2+}. PI3K and Akt activation led to the phosphorylation and inactivation of the positive cytokine regulator glycogen synthase kinase $3\alpha/\beta$ (GSK-$3\alpha/\beta$). PI3K, Akt, and mTOR inhibitors and small interfering RNA knockdown of Akt expression all increased, whereas a GSK-$3\alpha/\beta$ inhibitor decreased, Stx1-induced soluble tumor necrosis factor alpha and interleukin-1β production. Overall, these findings suggest that despite transient activation of 4E-BP, the PI3K/Akt/mTOR pathway negatively influences cytokine induction by inactivating the positive regulator GSK-$3\alpha/\beta$.

Bacteria producing Shiga toxins (Stxs), a family of functionally related AB_5 toxins, continue to be a significant public health concern. After ingestion of contaminated foods or water, the bacteria colonize the large intestine and cause bloody diarrhea with the potential to progress to life-threatening systemic complications including acute renal failure and central nervous system complications (45). The toxins are internalized and transported via the *trans*-Golgi network and Golgi apparatus to the endoplasmic reticulum (ER) and finally into the cytoplasm (39). It is well established that Stxs are protein synthesis inhibitors. Toxin A subunits mediate protein synthesis inhibition by depurination of a single adenine residue located on a stem-loop structure near the 3′ end of 28S rRNA of the 60S ribosomal subunit (11, 41). The toxins bind cells through interaction of pentameric B subunits with the neutral membrane glycolipid globotriaosylceramide (Gb3) (28).

In addition to protein synthesis inhibition, it has become clear that Stxs also activate host cell signaling pathways involved in the induction of cytokine and chemokine expression (3, 5, 20, 34, 51). Among the cytokines induced by Stxs, tumor necrosis factor alpha (TNF-α) and interleukin-1β (IL-1β) increase Gb3 expression on human vascular endothelial cells in vitro (35, 50). Thus, the host innate immune response to the toxins may participate in the development of intestinal, renal,

and central nervous system vascular lesions characteristic of bloody diarrhea and postdiarrheal sequelae. A more complete understanding of the signaling mechanisms activated by Stxs will be important for the development of therapeutic approaches for treating this emerging infectious disease. The precise cellular sources of cytokines in patients with bloody diarrhea or systemic complications are unknown. However, macrophages produce soluble cytokines and chemokines in response to microbes and microbial products. Furthermore, monocytic infiltration of the lamina propria and renal interstitial spaces was observed in animals administered Stxs (23, 46). Stxs regulate cytokine expression by human macrophage-like THP-1 cells through transcriptional and translational mechanisms. Transcriptional regulation involves prolonged activation of the stress-associated protein kinases p38 and Jun N-terminal protein kinase (JNK), transient activation of extracellular signal-regulated kinases 1 and 2 (ERK1/2), and activation of the transcription factors NF-κB and AP-1 (5, 38). Toxin-mediated translational control of cytokine expression involves, in part, stabilization of cytokine and chemokine mRNA transcripts (19, 20, 49).

In eukaryotic cells, initiation is the rate-limiting step controlling translation (37). Initiation involves modulation of protein-protein and protein-RNA interactions and is under the control of diverse signal transduction pathways, including mitogen-activated protein kinases (MAPKs) (25, 42). Translation initiation begins with the formation of eIF4F, a 43S preinitiation complex containing the 40S rRNA subunit, eukaryotic initiation factors (eIFs), and Met-tRNA (17). Formation of this complex depends on activation (phosphorylation) and availability of initiation factor 4E (eIF4E) following release

---

* Corresponding author. Mailing address: Department of Microbial and Molecular Pathogenesis, College of Medicine, 407 Reynolds Medical Building, Texas A&M University System Health Science Center, College Station, TX 77843-1114. Phone: (979) 845-1313. Fax: (979) 845-3479. E-mail: tesh@medicine.tamhsc.edu.

from cytosolic sequestering proteins called 4E-binding proteins (4E-BPs). Treatment of macrophage-like THP-1 cells with Shiga toxin 1 (Stx1) resulted in increased eIF4E activation, and inhibitors that blocked toxin-induced eIF4E activation diminished cytokine production (5). The affinity of 4E-BPs for eIF4E is regulated by the phosphorylation status of at least six 4E-BP serine/threonine residues (T37, T46, S65, T70, S83, and S112), with 4E-BP hyperphosphorylation associated with eIF4E release. In response to signals such as growth factors, 4E-BPs appear to be phosphorylated in a stepwise manner, with phosphorylation of the amino-terminal T37 and T46 residues functioning as a priming step for subsequent phosphorylation events (16). Following 4E-BP hyperphosphorylation at S65 and T70, released eIF4E may be phosphorylated and bind to the 5′-methylguanosine (m^7GpppN, where N is any nucleotide) cap of mRNA transcripts to initiate translation. In mammalian cells, 4E-BP hyperphosphorylation is regulated in part by signaling through phosphatidylinositol 3-kinase (PI3K), Akt (or protein kinase B), and mammalian target of rapamycin (mTOR) (15, 30). The influence of the PI3K/Akt/mTOR pathway on cytokine expression has been reported to be positive or negative depending on the cytokine and cell type studied (18, 31). Pathways regulating Stx-induced 4E-BP activation and eIF4E release are not well understood. In this study, we have shown that Stx1 treatment of THP-1 cells results in transient 4E-BP hyperphosphorylation. Stx1 signals 4E-BP activation through the PI3K/Akt/mTOR pathway, and a toxin enzymatic mutant appears to partially activate this pathway. Stx1 treatment triggered increased cytosolic Ca^{2+} levels and phosphorylation (inactivation) of the positive cytokine regulator glycogen synthase kinase 3α/β (GSK-3α/β). We examined the role of Stx1-induced PI3K/Akt/mTOR signaling in cytokine production. Inhibitors of the PI3K/Akt/mTOR pathway and small interfering RNA (siRNA) knockdown of Akt expression increased, while a GSK-3α/β inhibitor decreased, production of TNF-α and IL-1β 24 h after Stx1 treatment, suggesting that despite triggering the transient activation of 4E-BPs, the PI3K/Akt/mTOR pathway primarily plays a negative role in regulating cytokine production.

MATERIALS AND METHODS

Antibodies and reagents. Rabbit anti-human PI3K phospho-p85 antibody was from Santa Cruz Biotechnology Inc. (Santa Cruz, CA). Anti-human phospho-4E-BP, anti-phospho-Akt, anti-phospho-GSK-3α/β antibodies, Akt kinase assay kits, and Akt siRNA were from Cell Signaling Technology (Beverly, MA). The fluorescent calcium indicator Fluo-5F acetoxymethyl ester (AM) was obtained from Molecular Probes, Inc. (Eugene, OR). The PI3K inhibitors wortmannin and LY294002, Akt kinase inhibitor VIII, mTOR inhibitor rapamycin, JNK inhibitor SP600125, p38 MAPK inhibitor SB203580, ERK1/2 inhibitor PD98059, and GSK-3α/β inhibitor IX were purchased from Calbiochem (San Diego, CA). TNF-α and IL-1β enzyme-linked immunosorbent assay (ELISA) kits were from R&D Systems Inc., Minneapolis, MN. Immunoprecipitation kits were purchased from Amersham Pharmacia Biotech (Piscataway, NJ). All other reagents were obtained from Sigma Chemical Co. (St. Louis, MO).

Toxins. Stx1 was purified as described previously (47). Briefly, *Escherichia coli* DH5α(pCKS112) expressing the stx_1 operon was grown in Luria-Bertani broth with ampicillin. Stx1 was purified from cell lysates by sequential ion exchange, chromatofocusing, and immunoaffinity chromatography. The purity of toxins was tested by sodium dodecyl sulfate-polyacrylamide gel electrophoresis (SDS-PAGE) with silver staining and Western blot analysis with anti-Stx1 monoclonal antibody. Endotoxin levels in toxin preparations contained <0.1 ng of endotoxin per ml as determined by the *Limulus* amoebocyte lysate assay (Associates of Cape Cod, East Falmouth, MA). Purified Stx1 holotoxin containing a double

mutation (E167Q and R170L) in the A subunit which dramatically reduces enzymatic activity (32) was the kind gift of Shinji Yamasaki, Osaka Prefecture University (Osaka, Japan). Purified Stx1 B subunit was the kind gift of Cheleste Thorpe, Tufts University New England Medical Center (Boston, MA). Purified lipopolysaccharides (LPS) derived from *E. coli* O111:B4 were purchased from Sigma.

Cell culture and differentiation. The human myelogenous leukemia cell line THP-1 was purchased from American Type Culture Collection (Rockville, MD) and cultured in RPMI-1640 medium (Gibco-BRL, Grand Island, NY) supplemented with penicillin (100 U/ml), streptomycin (100 μg/ml), and 10% fetal bovine serum (HyClone Laboratories, Logan, UT; or Gemini Bioproducts, West Sacramento, CA). Cells were grown and maintained at 37°C in 5% CO_2 in a humidified incubator. To differentiate THP-1 cells to the adherent, macrophage-like state, cells were incubated with phorbol 12-myristate 13-acetate (50 ng/ml) for 48 h. The medium was then replaced with medium lacking phorbol 12-myristate 13-acetate, with daily medium changes, for 3 days prior to use of the cells in experiments.

Preparation of cell lysates, immunoprecipitation, and Western blot analysis. THP-1 cells (5×10^6 cells/ml) were washed in cold Dulbecco's phosphate-buffered saline (PBS) and cultured in RPMI-1640 with 0.5% fetal bovine serum (FBS) for 18 h to reduce endogenous kinase activity. Cells were stimulated with Stx1, an Stx1 enzymatic mutant (Stx1A⁻; 400 ng/ml), or purified Stx1 B subunits (800 ng/ml). We previously reported that this Stx1 concentration resulted in a transient increase in total protein synthesis by THP-1 cells lasting 2 h, after which protein synthesis decreased (12). Cells were harvested and lysed at 4°C in modified radioimmunoprecipitation assay buffer (1.0% Nonidet P-40, 1.0% Na deoxycholate, 150 mM NaCl, 1 mM Na_2EDTA, 50 mM Tris-HCl [pH 7.5], 0.25 mM Na pyrophosphate, 2.0 mM [each] sodium vanadate [$NaVO_4$] and sodium fluoride [NaF], 10 μg/ml aprotinin, 1.0 μg/ml leupeptin and pepstatin, and 200 mM phenylmethylsulfonyl fluoride). Extracts were collected and cleared by centrifugation at $15,000 \times g$ for 10 min. Cleared extracts were stored at −80°C until used. The protein content in cell extracts and cytosolic fractions prepared from stimulated THP-1 cells was determined using the DC protein assay kit (Bio-Rad, Hercules, CA). For immunoprecipitation reactions, extracts containing 300 μg protein were precleared with 20 μl protein A:G (equal ratio) for 1 h. Anti-p85 antibody was added, with incubation overnight. Then, 20 μl of protein A:G was added for 2 h. Beads were pelleted by centrifugation, washed three times, and boiled with 2× sample buffer. Proteins were separated by 8% SDS-PAGE. For Western blotting, equal amounts of proteins (60 to 80 μg protein per gel lane) were separated by 8% or 12% Tris-glycine SDS-PAGE and transferred to nitrocellulose membranes. Membranes were blocked with 5% milk prepared in TBST (20 mM Tris [pH 7.6], 137 mM NaCl, containing 0.1% Tween 20) and incubated with primary antibodies specific for 4E-BP, PI3K phospho-p85, or Akt in 5% bovine serum albumin in Tris-buffered saline and 0.1% Tween 20 overnight at 4°C and then with corresponding secondary antibodies (anti-rabbit/mouse immunoglobulin G [IgG] coupled to horseradish peroxidase [HRP]) for 2 h at room temperature. Bands were visualized using the Western Lightning chemiluminescence system (NEN-Perkin Elmer, Boston, MA).

Analysis of eIF4E and 4E-BP dissociation. m^7GTP-Sepharose 4B was obtained from Amersham Pharmacia Biotech (Piscataway, NJ). THP-1 cells (1.0×10^7 cells/ml) were washed and stimulated as described above. Cells were lysed at 4°C in lysis buffer (1% Nonidet P-40, 0.25% Na deoxycholate, 150 mM NaCl, 50 mM HEPES [pH 7.5], 25 mM glycerol phosphate, 2.0 mM [each] $NaVO_4$, NaF, and EDTA, 10 μg/ml aprotinin, 1.0 μg/ml leupeptin and pepstatin, and 200 mM phenylmethylsulfonyl fluoride). Extracts were collected and cleared by centrifugation at $15,000 \times g$ for 10 min. The protein content in cell extracts was determined using the DC protein assay kit (Bio-Rad, Hercules, CA). Equal amounts of protein (300 μg) were precleared with Sepharose 4B (30 μl of settled bed volume) for 1 h, and then an equal volume of m^7GTP-Sepharose 4B was added with incubation at 4°C overnight with gentle shaking. Precipitates and supernatants were collected. Precipitates were washed three times with lysis buffer, and proteins from precipitates or supernatants were separated by 15% SDS-PAGE. Western blotting was performed with anti-phospho-eIF4E and anti-rabbit IgG-HRP antibodies. For loading controls, the same blots were stripped and reprobed with antibodies against total eIF4E. The same samples were run in parallel for blotting with various anti-phospho-4E-BP antibodies.

Akt kinase activity assay. Akt kinase activity was determined using kits purchased from Cell Signaling Technology according to the manufacturer's instructions. Briefly, THP-1 cells (5×10^6 cells/ml) were untreated or treated with Stx1 (400 ng/ml), washed with ice-cold PBS, and lysed with ice-cold lysis buffer provided with the kit. Samples were incubated for 20 min on ice. Cell lysates were centrifuged, and supernatants were obtained. Protein concentrations were measured using Bio-Rad DC protein assay kits. Equal amounts of protein (300 μg)
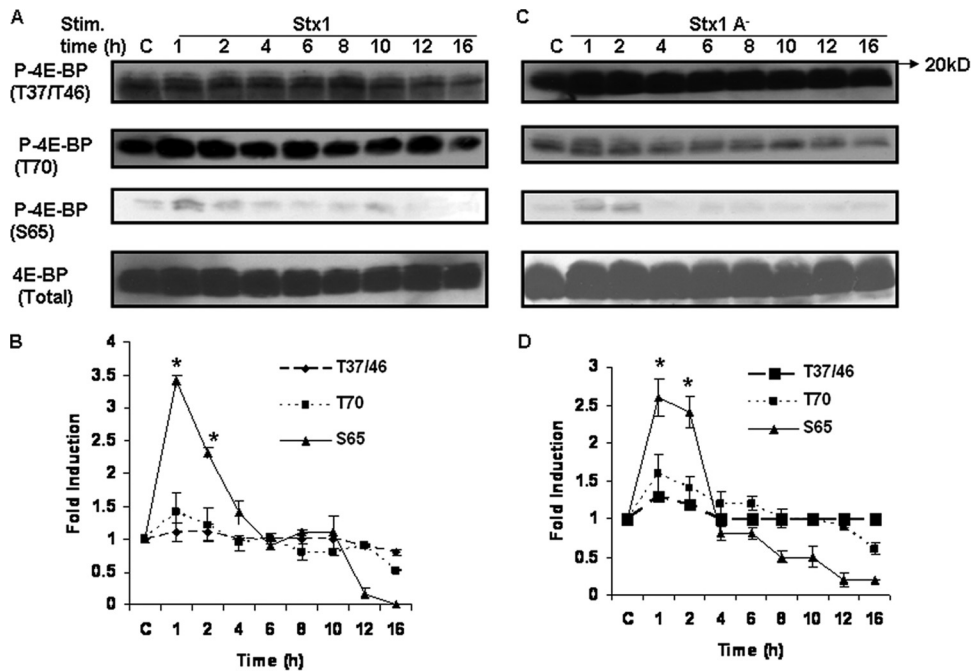
FIG. 1. Stx1 induces transient 4E-BP phosphorylation at serine 65 in THP-1 cells. Adherent macrophage-like THP-1 cells were stimulated with Stx1 (A) or Stx1A⁻ (C) (400 ng/ml) for 1 to 16 h (Stim. time). Cell lysates were prepared and Western blotting performed using site-specific antibodies for 4E-BP phosphothreonine or phosphoserine residues. Blots were stripped and reprobed with antibodies against total 4E-BP to control for equal protein loading (bottom panels). C, lysates prepared from control cells maintained for 16 h without toxin. Band intensities from at least four independent experiments using Stx1 (B) or Stx1A⁻ (D) were measured by densitometry, and the data are expressed as mean *n*-fold changes ± SEM relative to results for untreated control cells. Asterisks (∗) denote significant differences ($P < 0.05$) versus results for control cells.

were precleared with protein A-protein G (1:1) Sepharose. Immobilized anti-Akt monoclonal antibody agarose was added and incubated at 4°C overnight with gentle shaking. Immunoprecipitates were washed three times with lysis buffer and twice with Akt kinase buffer containing 200 μM ATP and 1.0 μg GSK-3β fusion protein. The sample proteins were separated by 12% SDS-PAGE, and Western blotting was performed with anti-phospho-GSK-3α/β and anti-rabbit IgG-HRP antibodies. Band intensities were quantified and induction calculated as the stimulated protein band intensity values divided by unstimulated control protein band intensity values after normalizing for loading controls.

Calcium (Ca^{2+}) measurement. Fluo-5F AM, a cell-permeable fluorescent indicator of intracellular Ca^{2+} with an excitation wavelength of 488 nm and emission at 530 nm, was used. Fluo-5F AM has a relatively low Ca^{2+}-binding affinity, making it suitable for detecting intracellular Ca^{2+} levels in the range of 1.0 μM to 1.0 mM. Low Ca^{2+}-binding affinities are ideal for detecting high concentrations of Ca^{2+} released from ER stores (22, 33). Differences in fluorescence, with or without toxin treatment, were measured using the Zeiss Stallion live cell imaging system (Carl Zeiss Microscopy, Gottingen, Germany) equipped with an argon laser. The cells were incubated with Fluo-5F AM (3.0 μM) for 45 min at 37°C and 5% CO_2. Basal fluorescence was measured for 10 min. Cells were then stimulated with Stx1 (400 ng/ml) and fluorescence measurements continued for 1 h. Finally, fluorescence was measured after adding the ER-localized Ca^{2+}-dependent ATPase inhibitor thapsigargin (10 μM) for 10 min. Fluorescence intensity was measured in the presence of Ca^{2+}-containing medium and Ca^{2+}-free medium (made by adding 2.0 mM EGTA) to identify intracellular and extracellular sources of Ca^{2+}. Normalized fluorescence intensity (from unstimulated cells) was plotted against time from three independent experiments.

ELISA for soluble TNF-α and IL-1β production. Cell supernatants were collected from adherent THP-1 cells (2 × 10⁶ cells/ml) stimulated with Stx1 (400 ng/ml) for 24 h with or without pretreatment for 1 h with wortmannin, Akt inhibitor VIII, rapamycin, or GSK-3α/β inhibitor IX. Supernatants for TNF-α and IL-1β detection were added in duplicate wells to ELISA plates (R&D Systems) and the assay performed according to the manufacturer's protocol. Absorbance was measured at 450 nm and 570 nm using a microtiter plate reader (Dynatech MR5000; Dynatech Laboratories, Chantilly, VA). Mean cytokine

values (pg/ml) from three independent experiments were calculated and expressed as means ± standard errors of the means (SEM).

siRNA transfection. THP-1 cells (2 × 10⁶ cells/well) were differentiated in 12-well plates as described above. Two hours before transfection, medium was replaced with Dulbecco's modified Eagle medium plus 10% FBS. Complexes of transfection reagent and Akt-specific and nonspecific siRNAs were prepared according to the manufacturer's instructions (*Trans*IT-TKO transfection reagent; Mirus Bio Corporation, Madison, WI). After addition of the siRNA complexes, cells were incubated for 48 h at 37°C in 5% CO_2. Two hours before Stx1 stimulation, viable cells were washed with 1× PBS, and RPMI plus 10% FBS was added to the cells. Cells were treated with Stx1 for 24 h. Supernatants were collected for measurement of soluble cytokines by ELISA. Data are expressed as mean cytokine values (pg/ml) ± SEM from at least three independent experiments. To assess transfection efficiency, cell lysates were prepared and Western blotting performed using antibodies directed against total Akt and actin.

Statistical analyses. For statistical analysis of kinetic data for 4E-BP, PI3K, and phospho-p85 activation, Akt kinase assays, and cytokine expression, significance was calculated using Student's *t* test (Excel, Microsoft Corp., Redmond, WA). For Ca^{2+} measurements, a one-tailed simple *t* test with Welch's correction was used for calculation of significance. For Ca^{2+} measurements in the presence of EGTA, analysis of variance followed by Tukey's multiple comparison test was used for calculating significance. Significance was defined as a *P* value of <0.05.

RESULTS

Stx1 induces transient phosphorylation of 4E-BP at serine 65. Sequential phosphorylation of 4E-BP at multiple threonine and serine residues is necessary for the release eIF4E, which may lead to increased formation of translation initiation complexes and translation of mRNA transcripts. To examine whether Stxs induce sequential phosphorylation of 4E-BP, macrophage-like THP-1 cells were stimulated with purified
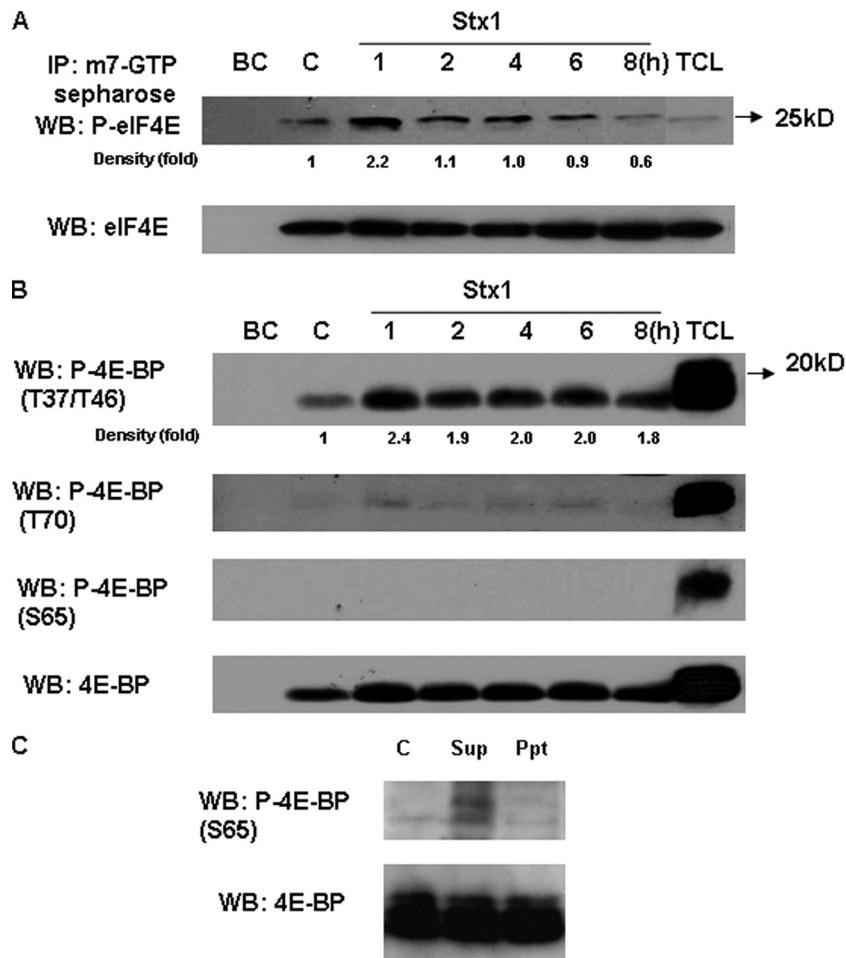
FIG. 2. Stx1 induces the dissociation of eIF4E from 4E-BP. Cell lysates from Stx1-treated THP-1 cells were incubated with m⁷GTP-Sepharose 4B beads. Beads were washed and Western blotting (WB) performed using antibodies specific for phosphorylated and total eIF4E (A) or phosphorylated 4E-BP and total 4E-BP (B) in immunoprecipitates. (C) Western blotting of phosphorylated 4E-BP (S65) and total 4E-BP in supernatants versus bead-containing immunoprecipitates. BC, bead control without cell lysates; C, control (unstimulated) cells; TCL, total cell lysates; Sup, supernatants; Ppt, immunoprecipitates. Band intensities were measured by densitometry, and n-fold changes are expressed beneath each lane. The data shown are representative of at least three independent experiments.

Stx1, mutated Stx1 holotoxin molecules with dramatically reduced enzymatic activity (Stx1A⁻), or purified Stx1 B subunits. At various time points after treatment, cells were lysed and Western blotting performed using site-specific antiphosphothreonine or antiphosphoserine antibodies. Representative Western blots are shown in Fig. 1A and C, and mean band intensities derived from at least four independent experiments are shown in Fig. 1B and D. 4E-BP appeared to be constitutively phosphorylated at positions T37, T46, and T70 in control (unstimulated) cells. Treatment with Stx1 failed to induce increased phosphorylation at T37 and T46 and caused only modest increases in T70 phosphorylation. In contrast, S65 was minimally phosphorylated in control cells, and in response to treatment with Stx1, 4E-BP was transiently phosphorylated at S65, peaking at a 3.4-fold increase 1 h after toxin treatment and declining over a 4-h time period (Fig. 1B). Blots were stripped and reprobed with anti-4E-BP antibody to ensure equal protein loading at each time point. Given the transient nature of 4E-BP activation by Stx1, we examined S65 phosphorylation 30 min after toxin treatment and failed to detect 4E-BP activation

(data not shown). Mutant Stx1A⁻ holotoxin failed to alter basal phosphorylation of 4E-BP at T37/46 but modestly increased T70 and significantly increased S65 phosphorylation, although peak activation levels were slightly less than that induced by Stx1 (Fig. 1D). Purified Stx1 B subunits also triggered 4E-BP phosphorylation at S65 (data not shown). These data suggest that toxin enzymatic activity may not be necessary for 4E-BP hyperphosphorylation.

Stx1 induces the dissociation of phospho-eIF4E and hyperphosphorylated 4E-BP. To show that Stx1-mediated 4E-BP hyperphosphorylation leads to eIF4E dissociation, we performed an affinity precipitation assay using m⁷GTP-Sepharose 4B beads. At various time points after toxin stimulation, cell lysates were incubated with the beads and precipitates were collected and analyzed by SDS-PAGE and Western blotting with phospho-specific antibodies against eIF4E and 4E-BP. As shown in Fig. 2A, upper panel, there was an increased association of phospho-eIF4E with m⁷GTP-coated beads after 1 h of toxin treatment, suggesting a transient dissociation from 4E-BP and increased binding to the 5′-cap structure of
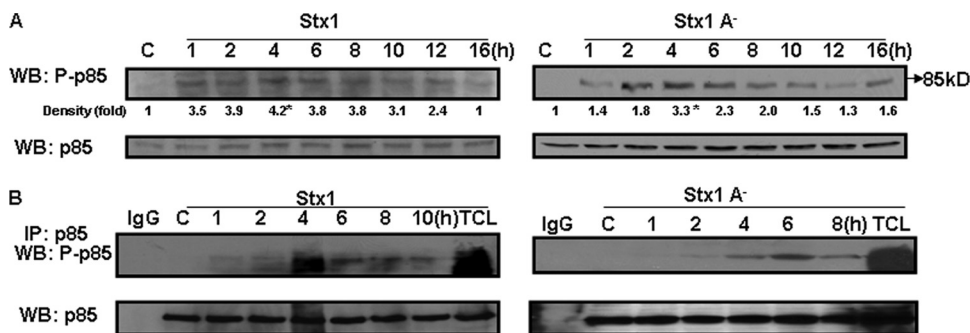
FIG. 3. Stx1 activates PI3K. (A) Adherent macrophage-like THP-1 cells were stimulated with Stx1 or inactive Stx1 holotoxin (Stx1A⁻) for 1 to 16 h. Cell lysates were prepared and Western blotting (WB) performed using antibodies specific for the phospho-p85 subunit of PI3K. Blots were stripped and reprobed with antibodies against p85 PI3K for equal protein loading (bottom panels). C, lysates prepared from control cells maintained for 16 h without toxin. Band intensities were measured by densitometry, and n-fold changes are expressed beneath each lane. Asterisks (∗) denote significant differences ($P < 0.05$) for results with toxin treatment versus results for control cells. (B) Immunoprecipitation reactions using anti-p85 PI3K antibodies were carried out with lysates prepared from Stx1- or Stx1A⁻ mutant-treated cells. Immunoprecipitates were separated by SDS-PAGE, transferred to nitrocellulose, and probed using anti-phospho-p85 PI3K antibodies. C, control (unstimulated) cells; IgG, antibody-only control; TCL, total cell lysates. Results shown are representative of at least three independent experiments.

mRNAs. Nonphosphorylated forms of eIF4E also bound the beads, but differences in binding were not manifest over prolonged exposure of the cells to toxin (Fig. 2A, lower panel). The data also showed that 4E-BP phosphorylated at the priming residues was associated with the m⁷GTP beads and eIF4E (Fig. 2B, upper panel). However, 4E-BP phosphorylated at T70 was only faintly detected, and S65 was not detected, in the precipitates. Western blots of cell lysate supernatants showed that hyperphosphorylated 4E-BP remained in the supernatant and was not associated with the precipitates pulled down by m⁷GTP beads (Fig. 2C). These data suggest that Stx1-induced phosphorylation of 4E-BP at positions T70 and S65 is necessary for eIF4E dissociation and m⁷GTP binding.

Stx1 activates PI3K. We have shown that eIF4E phosphorylation requires the internalization and transport of enzymatically active Stx1 and activation of the ribotoxic stress response (5). Many growth factors and hormones regulate translation by altering 4E-BP phosphorylation in a wortmannin- and rapamycin-sensitive manner, indicating that PI3K, Akt, and mTOR are involved in signaling pathways leading to 4E-BP activation (30). To test the hypothesis that in addition to initiating the ribotoxic stress response, Stx1 also initiates signaling through the PI3K/Akt/mTOR pathway, we examined PI3K activation in THP-1 cells treated with Stx1, an Stx1A⁻ mutant, or Stx1 B subunits. Cell lysates were analyzed for PI3K activation using an antibody directed against the phosphorylated p85 subunit by Western blotting and immunoprecipitation. Immunoblots were stripped and reprobed with total p85 antibody to ensure equal protein loading at each time point. Stx1 rapidly induced PI3K activation, with a 3.5-fold increase in activation at 1 h, which peaked after 4 h, followed by a decline to basal (unstimulated) levels over 16 h (Fig. 3A). The A-subunit mutant induced a 3.3-fold increase at 4 h posttreatment. Purified Stx1 B subunits stimulated a 3.5-fold increase in PI3K activation with similar kinetics (data not shown). To verify the capacity of Stx1 to functionally activate PI3K, we performed immunoprecipitation-Western analyses of lysates prepared from Stx1- or Stx1A⁻ mutant-treated cells. In this assay, the p85 subunit of PI3K is immunoprecipitated using anti-p85 antibodies, and the

immunoprecipitates are transferred to nitrocellulose membranes and probed with anti-phospho-p85-specific antibodies. Immunoprecipitates prepared from Stx1- and Stx1A⁻-treated cells showed increased levels of activated PI3K, peaking 4 to 6 h after toxin treatment (Fig. 3B). These data suggest that while enzymatically active Stx1 may mediate optimal PI3K activation, the binding or internalization of Stx1A⁻ or Stx1 B subunits may be sufficient to partially activate PI3K.

Stx1 induces increased cytosolic Ca²⁺ levels. PI3K activation leads to the production of phospholipid second messenger phosphatidylinositol-3,4,5-triphosphate, which may lead to Ca²⁺ release from ER stores after binding to ER membrane phosphatidylinositol-3,4,5-triphosphate receptors (2). We reasoned that Stx1-induced PI3K activation would result in increased cytosolic Ca²⁺ levels. We investigated Stx1-induced release of Ca²⁺ using the fluorescent calcium indicator Fluo-5F AM, which is a cell-permeable, relatively low-Ca²⁺-binding affinity marker suitable for measuring higher concentrations of Ca²⁺ released from ER stores. After 10 min of fluorescence measurements to establish basal intensity, the addition of Stx1 or Stx1A⁻ is shown in Fig. 4A or C, respectively. A slow but statistically significant (Fig. 4B and D) increase in fluorescence intensity up to 1 h after toxin treatment was detected. This slow increase in cytosolic Ca²⁺ levels was not detected in control (unstimulated) cells (data not shown). Addition of the positive control thapsigargin, a compound that prevents the uptake of cytosolic Ca²⁺ into the ER, is also shown in the figure. Increased fluorescence intensity was noted after thapsigargin treatment, implicating the ER as the source of intracellular Ca²⁺. To examine the influx of extracellular Ca²⁺, we measured fluorescence in cells treated with Stx1 (Fig. 4E) or Stx1A⁻ (Fig. 4G) maintained in Ca²⁺-chelated (EGTA) medium. In the presence of EGTA, there was a sharp increase in fluorescence intensity when Stx1 was added, and cytosolic Ca²⁺ levels increased with thapsigargin treatment. However, significant continual increases in cytosolic Ca²⁺ were not detected after 1 h of toxin treatment when cells were maintained in chelated medium (Fig. 4F and H). These data indicate that Stx1 stimulation activates PI3K and Ca²⁺ release
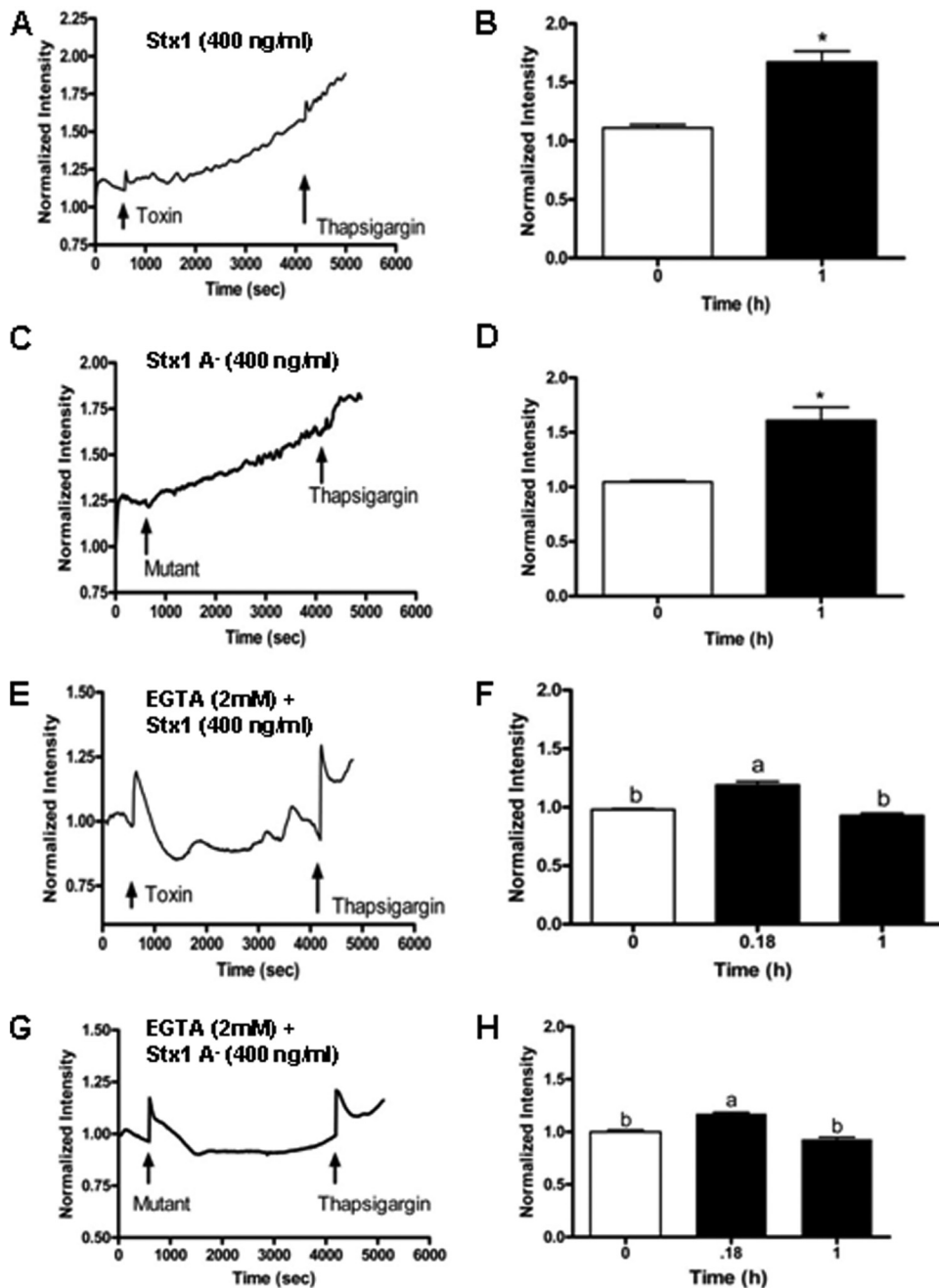
FIG. 4. Stx1 triggers increased cytosolic Ca^{2+} levels in THP-1 cells. THP-1 cells were maintained in Ca^{2+}-containing medium and then treated with the fluorescent Ca^{2+} indicator Fluo-5F. Basal cytosolic Ca^{2+} levels were determined for 10 min using the Zeiss Stallion live cell imaging system. The first arrows indicate the addition of Stx1 (A) or (C) Stx1A$^-$ to the cells. After measurement of Ca^{2+} levels for 1 h, thapsigargin was added to the cells (second arrows). Fluorescence intensities at 0-h time points and 1 h after Stx1 (B) or Stx1A$^-$ (D) treatments were plotted for three independent experiments. Asterisks ($*$) indicate statistically significant differences ($P < 0.05$) in cytosolic Ca^{2+} levels. To examine the uptake of extracellular Ca^{2+}, THP-1 cells were maintained in Ca^{2+}-chelated medium prior to the addition of Fluo-5F and Stx1 (E) or Stx1A$^-$ (G). Changes in intracellular Ca^{2+} were measured as outlined above. (F and H) Statistical analysis of differences in cytosolic Ca^{2+} levels at 0, 0.18, and 1 h after Stx1 or Stx1A$^-$ treatment. a, statistically significant difference ($P < 0.05$); b, not significant.

in THP-1 cells. Sources of increased cytosolic Ca^{2+} may include the ER, but we cannot rule out additional influx from the extracellular environment.

Stx1 activates Akt. Following phosphorylation of membrane-associated phosphatidylinositol second messengers by PI3K, a number of signaling pathways are activated, including the serine/threonine kinase Akt (13). Akt is phosphorylated at two sites, S308 by phosphatidylinositol-dependent kinase 1 (PDK1) and S473 by mTOR (40). Treatment of THP-1 cells with Stx1 resulted in transient Akt phosphorylation at S473 (Fig. 5A), suggesting that mTOR activation by Stx1 is likely. Akt activation peaked at a 6.8-fold increase 6 h after toxin
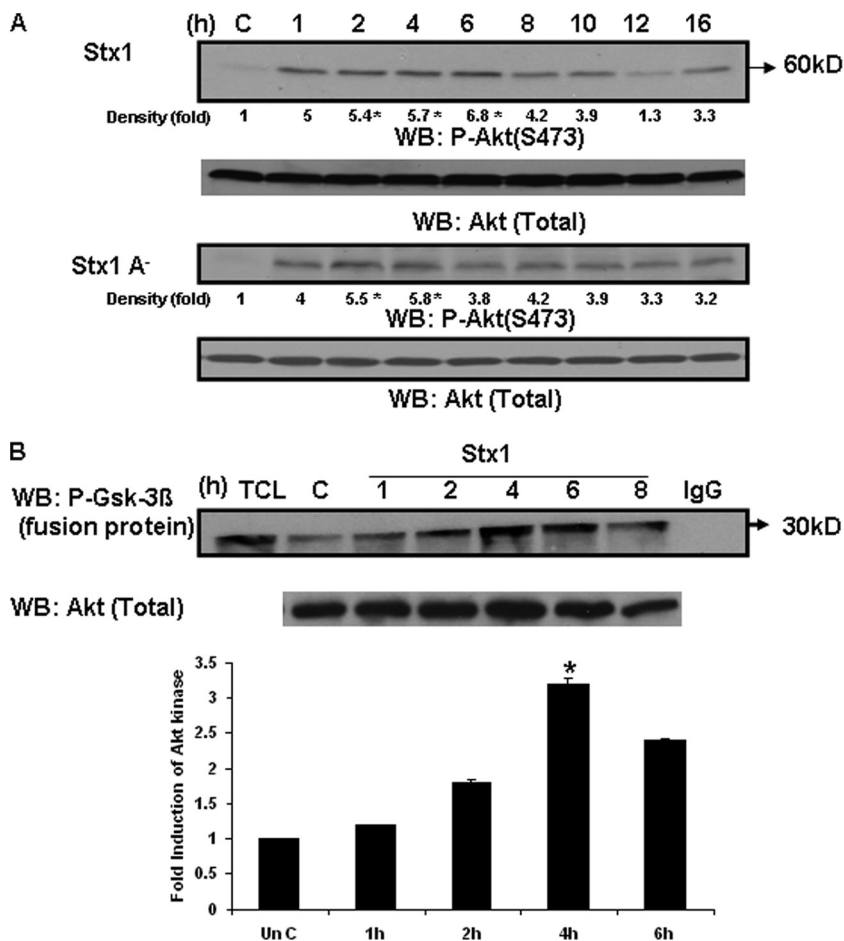
FIG. 5. Stx1 and Stx1A$^-$ activate Akt in THP-1 cells. (A) THP-1 cells were stimulated with Stx1 or Stx1A$^-$ for 1 to 16 h. At each time point, cell lysates were prepared and Western blotting (WB) performed using antibodies specific for phospho-Akt (S473). Blots were stripped and reprobed with antibodies recognizing total Akt for equal protein loading (bottom panel). C, lysates prepared from control cells maintained for 16 h without Stx1. Band intensities were measured by densitometry, and n-fold changes are expressed beneath each lane. (B) THP-1 cells were treated with Stx1 for 1 to 8 h. At each time point, cell lysates were prepared. Supernatants collected from the lysates were precleared and incubated with an anti-Akt monoclonal antibody. An Akt kinase assay was performed with the resultant immunoprecipitates using a synthetic GSK-3β fusion protein substrate in the presence of ATP. Proteins were then separated by SDS-PAGE and Western blotting performed using an antibody recognizing phospho-GSK-3β. A representative Western blot is shown in the upper panel. TCL, total cellular lysate; C, lysates from control (unstimulated) cells; IgG, negative control. The bar graph shown in the lower panel is the n-fold-induction of Akt kinase activity following Stx1 treatment of THP-1 cells derived from at least three independent experiments. Asterisks (∗), significant difference ($P < 0.05$) for toxin treatment results versus those with control cells.

administration and returned to basal levels 12 h after toxin treatment. Stx1A$^-$ also activated Akt, with similar kinetics. All immunoblots were stripped and probed with antibody recognizing total Akt protein as a control for equal protein loading. To ensure that treatment of THP-1 cells with Stx1 resulted in the activation of functional Akt, we immunoprecipitated Akt from cell lysates, and the resultant immune complexes were used in a kinase assay measuring phosphorylation of a synthetic GSK-3β fusion protein as a substrate (P-GSK-3β fusion protein; Fig. 5B). Stx1 treatment of THP-1 cells resulted in a 3.2-fold increase in Akt kinase function at 4 h with kinetics closely corresponding to that of Akt phosphorylation shown in Fig. 5A.

PI3K and Akt inhibitors block 4E-BP phosphorylation. To link Stx1-induced PI3K and Akt activation with 4E-BP phosphorylation, THP-1 cells were treated with various concentra-

tions of wortmannin, LY294002, or Akt inhibitor VIII for 1 h prior to stimulation with Stx1. Cell lysates were prepared and 4E-BP phosphorylation status determined by Western blotting using phospho-T37/46-, -S65-, or -T70-specific anti-4E-BP antibodies. Equal protein loading was determined using anti-4E-BP antibodies. Wortmannin at a 100 nM concentration (Fig. 6A) or LY294002 at 10 to 20 μM (data not shown) inhibited 4E-BP phosphorylation in Stx1-treated cells. Akt inhibitor VIII at 20 μM was also effective in blocking 4E-BP phosphorylation in Stx1-treated cells. Thus, signaling through PI3K and Akt appears necessary to maintain 4E-BP basal priming phosphorylation and for activation at T70 and S65 since the priming sites are necessary for subsequent phosphorylation events (16).

mTOR inhibitor blocks Stx1-induced 4E-BP hyperphosphorylation at T70 and S65. mTOR is a large (289-kDa) serine/
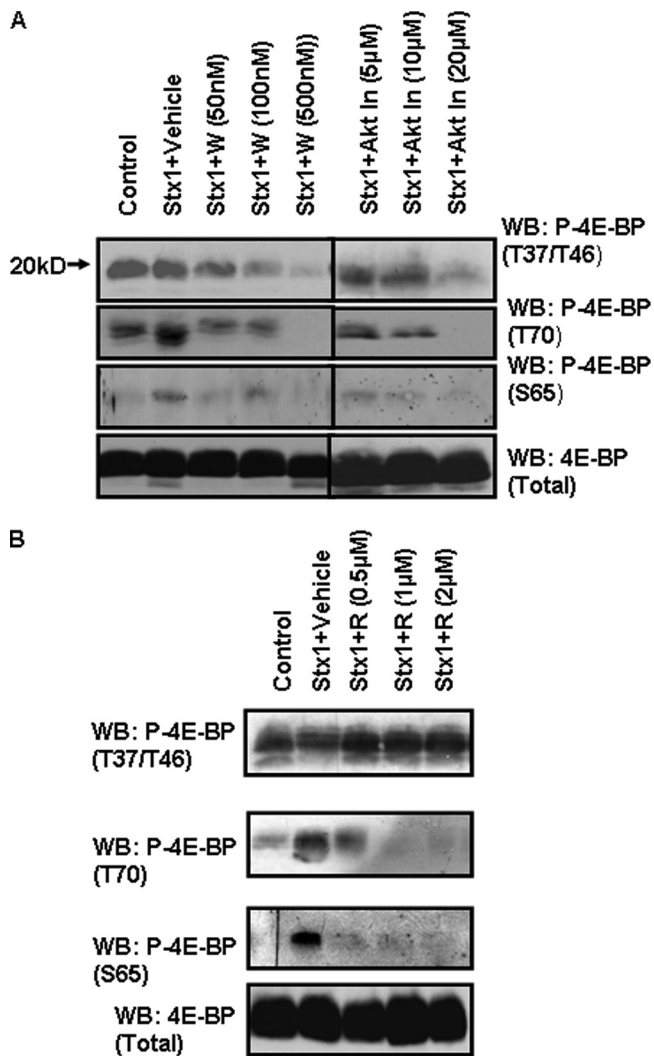
A

B

FIG. 6. PI3K, Akt, and mTOR inhibitors block 4E-BP phosphorylation. THP-1 cells were incubated with the indicated concentrations of PI3K inhibitor (wortmannin; W) or Akt Inhibitor VIII (Akt In) (A) or mTOR inhibitor rapamycin (R) (B) for 1 h prior to the addition of Stx1 (400 ng/ml) for 1 h. Lysates were prepared and Western blotting (WB) performed using antibodies recognizing phosphorylated 4E-BP residues T37 and T46, T70, and S65. Blots were stripped and reprobed with antibody recognizing total 4E-BP for equal protein loading. Control, unstimulated cells. The results shown are representative of at least three independent experiments.

threonine kinase which regulates both transcription and translation. mTOR is activated by growth factors and insulin in a PI3K-dependent manner. Akt directly phosphorylates mTOR at position S2448. The two major substrates of mTOR activity are p70S6K, a kinase involved in ribosome biogenesis, and 4E-BP (1). To demonstrate that mTOR is involved in Stx1-induced 4E-BP activation, THP-1 cells were treated with the mTOR inhibitor rapamycin for 1 h prior to stimulation with Stx1. Cell lysates were prepared and 4E-BP phosphorylation status determined by Western blotting (Fig. 6B). As expected, comparison of unstimulated control cells versus Stx1-stimulated cells showed that phosphorylation at the T37/T46 priming sites was not altered by toxin treatment. Rapamycin treat-

ment failed to alter phosphorylation at these residues in Stx1-treated cells (upper panel). In contrast, toxin treatment triggered 4E-BP phosphorylation at T70 (center panel) and S65 (lower panel), and rapamycin inhibited phosphorylation at these positions in a dose-dependent manner. Thus, mTOR is involved in signaling selectively regulating 4E-BP phosphorylation at T70 and S65.

MAPK cascades do not regulate 4E-BP phosphorylation. Treatment of THP-1 cells with Stx1 leads to the prolonged activation of MAPKs p38 and JNK, transient activation of ERK1/2, enhanced eIF4E phosphorylation, and the expression of cytokines (5). However, the activation of 4E-BP is reported to be mediated through the PI3K/Akt/mTOR pathway independently of MAPK cascades (52). To examine the roles of MAPKs in Stx1-induced signaling for 4E-BP activation, we treated cells with inhibitors of ERK, JNK, and p38 MAPK cascades or treated cells with all three inhibitors for 1 h prior to treatment with Stx1. Cell lysates were prepared and 4E-BP phosphorylation status ascertained by Western blotting using phospho-T37/46- and -S65-specific antibodies. None of the MAPK inhibitors altered Stx1-mediated 4E-BP phosphorylation (data not shown). Although Stx1 activates MAPK signaling cascades, these pathways do not appear to be involved in signaling for 4E-BP phosphorylation.

Stx1 activation of Akt results in phosphorylation of GSK-$3\alpha/\beta$. Akt activation leads to the activation or inactivation of a large number of substrates (43). Akt directly phosphorylates and inactivates GSK-$3\alpha/\beta$ on S9 or S21, respectively (10). To detect GSK-$3\alpha/\beta$ inactivation, THP-1 cells were treated with Stx1 for various time periods. Western blotting was then performed on lysates using anti-phospho-GSK-$3\alpha/\beta$ antibodies. Within 4 h of stimulation with Stx1, GSK-$3\alpha/\beta$ showed increased phosphorylation that was maintained up to 16 h after treatment (Fig. 7A). To examine the role of PI3K and Akt in toxin-mediated signaling leading to GSK-$3\alpha/\beta$ inactivation, we stimulated THP-1 cells with Stx1 in the presence of specific PI3K and Akt inhibitors. Changes in phospho-GSK-$3\alpha/\beta$ levels were measured by Western blotting (Fig. 7B). The PI3K inhibitor wortmannin inhibited GSK-$3\alpha/\beta$ phosphorylation at the lowest (50 nM) inhibitor concentration tested. The Akt inhibitor also blocked GSK-$3\alpha/\beta$ phosphorylation, with optimal inhibition noted at 20 μM. The inhibitors alone did not alter GSK-$3\alpha/\beta$ phosphorylation (data not shown). These data suggest that signaling through PI3K/Akt is essential for GSK-$3\alpha/\beta$ inactivation.

Role of PI3K/Akt/mTOR pathway in cytokine production. To study the role of the PI3K/Akt/mTOR pathway in cytokine expression, we observed the effects of PI3K, Akt, mTOR, and GSK-$3\alpha/\beta$ inhibitors on Stx1-induced soluble cytokine production by THP-1 cells (Fig. 8A and B). Cells were treated with wortmannin, Akt inhibitor VIII, rapamycin, or GSK-$3\alpha/\beta$ inhibitor IX for 1 h. To some cells, Stx1 was added and incubation continued for 24 h. Cell supernatants were collected for quantification of TNF-α and IL-1β. As previously reported, Stx1 treatment induced increased cytokine expression by THP-1 cells in vitro (34). PI3K/Akt/mTOR inhibitor treatments alone resulted in dose-dependent increases in TNF-α and IL-1β production compared to results for control (untreated) cells. However, cells pretreated with the inhibitors and Stx1 showed significant dose-dependent increases in cytokine
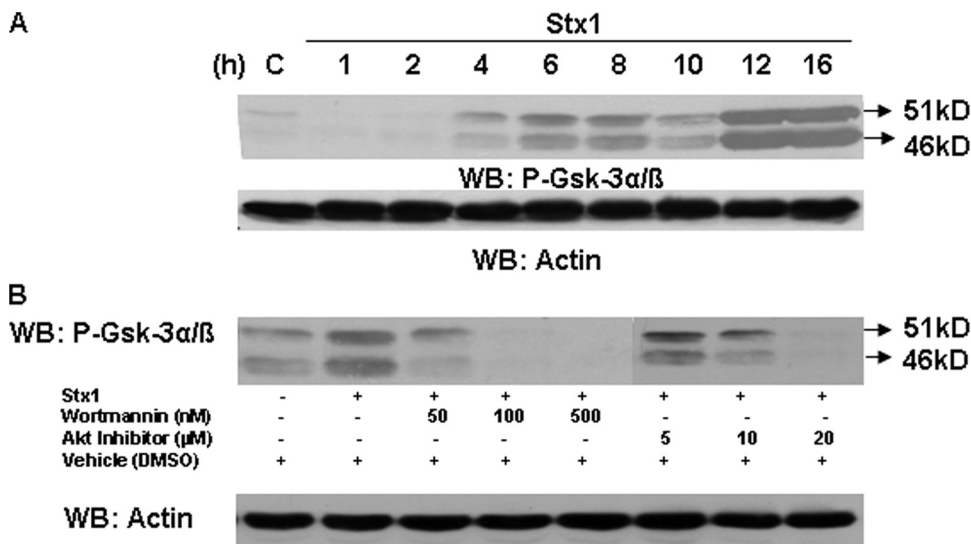
FIG. 7. PI3K/Akt activation by Stx1 results in the activation of the downstream substrate GSK-3α/β. (A) THP-1 cells were stimulated with Stx1, and at each time point, cell lysates were prepared and Western blotting (WB) performed using antibodies specific for phospho-GSK-3α/β. Blots were stripped and reprobed with antibodies recognizing actin for equal protein loading (bottom panel). C, lysates prepared from control cells maintained for 16 h without Stx1. (B) THP-1 cells were treated with the indicated amounts of PI3K (wortmannin) or Akt inhibitors for 1 h prior to stimulation with Stx1 for 1 h (PI3K inhibition) or 4 h (Akt inhibition). Cell lysates were prepared and Western blotting performed using antibodies specific for phospho-GSK-3α/β. Blots were stripped and reprobed with antibodies recognizing actin for equal protein loading (bottom panel). Results shown are representative of at least three independent experiments.

expression. In contrast, in cells treated with GSK-3α/β inhibitor IX and Stx1, we observed a 50% reduction in soluble TNF-α production and a 20% reduction in soluble IL-1β production compared to results for cells treated with Stx1 alone. Thus, 24 h after toxin treatment, the PI3K/Akt/mTOR pathway appears to negatively regulate soluble proinflammatory cytokine production by Stx1-treated THP-1 cells. The precise mechanism of negative regulation is unknown, but our data suggest that Stx1-induced PI3K/Akt/mTOR activation may decrease cytokine expression in part by blocking the action of a positive cytokine regulator, GSK-3α/β.

To confirm the data on the negative role of Akt in Stx1-induced cytokine expression using pharmacological inhibitors, we used siRNAs to knock down Akt expression. THP-1 cells were transfected with Akt-specific siRNA or nonspecific control siRNA for 48 h and were then stimulated with Stx1. The cells were lysed and Western blotting performed. We detected a 54% decrease in total Akt protein in cells transfected with Akt-specific siRNA normalized against actin levels (Fig. 9A). Cell supernatants prepared from all transfected cells were analyzed by ELISA for TNF-α and IL-1β expression (Fig. 9B and C). TNF-α and IL-1β production was increased 69% and 49%, respectively, in Akt siRNA-transfected cells. These data support a negative role for signaling through the Akt pathway in cytokine production.

DISCUSSION

Human adherent macrophage-like THP-1 cells respond to Stxs by induction and expression of proinflammatory cytokines (34). The localized expression of TNF-α and IL-1β may contribute to the pathogenesis of hemorrhagic colitis and acute renal failure, since these cytokines regulate expression of Gb3

biosynthetic genes leading to increased toxin receptor expression on endothelial cells (44). Prolonged expression of proinflammatory cytokines leads to pathological consequences. Therefore, cytokine expression is tightly regulated at transcriptional, translational, and posttranslational stages. Our studies suggest that Stxs regulate cytokine expression at multiple levels. Toxin-induced cytokine expression occurs, in part, through activation of the stress-associated protein kinases leading to activation of the transcriptional factors NF-κB and AP-1 (5, 38, 53). Translational control mechanisms may include changes in mRNA stability and translation initiation, alternative RNA splicing events, and RNA nucleocytoplasmic transport (14). Cytokine and chemokine mRNA transcripts induced by Stxs appear to be more stable than transcripts induced by LPS or TNF-α (19, 20, 49). The precise mechanisms by which Stxs stabilize mRNA transcripts remain to be characterized. However, a deadenylation-dependent 5' $\rightarrow$ 3' mRNA decay pathway is initiated following decapping of the 5'-m^{7}GpppN cap (7). Thus, translation rates of individual mRNAs may reflect the relative ability to assemble translational initiation complexes versus assembly of translational repression or degradation complexes at the 5' cap structure (8). In this regard, we have shown that treatment of THP-1 cells with Stx1 increases eIF4E phosphorylation through an ERK1/2- and p38 MAPK/Mnk1-dependent signaling cascade. MAPK and Mnk1 inhibitors reduce cytokine expression by THP-1 cells upon exposure to Stx1 (5). Collectively, these data suggest that Stxs may rapidly regulate cytokine production, in part, by increased efficiency of translation initiation and reduced transcript degradation by blocking of transcript decapping and decay.

The rate-limiting step in formation of the eIF4F complex is binding of eIF4E to the 5' cap. eIF4E activity is inhibited by a family of repressors called 4E-BP. In the partially phosphory-
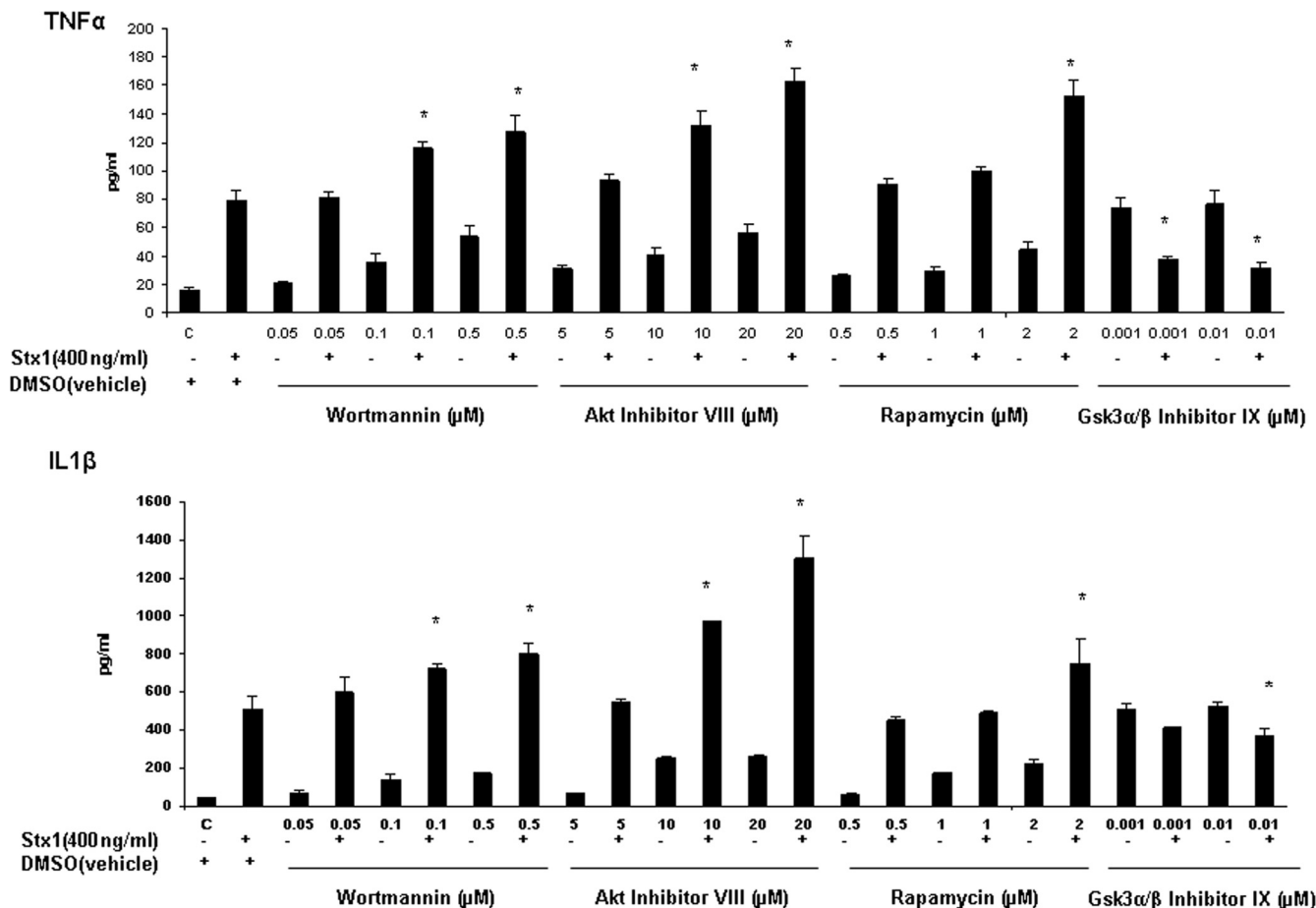
FIG. 8. Effect of pretreatment with PI3K (wortmannin), Akt (Akt inhibitor VIII), mTOR (rapamycin), or GSK-3α/β (GSK-3α/β inhibitor IX) inhibitor on Stx1-induced soluble TNF-α and IL-1β production. Differentiated THP-1 cells were treated with the inhibitors for 1 h, and Stx1 was added for 24 h. Cell supernatants were collected. Soluble TNF-α and IL-1β were quantified using ELISA kits. All values are expressed in pg/ml ± SEM. Asterisks (∗) represent significant differences ($P < 0.05$) between results with Stx1 treatment versus those with Stx1-plus-inhibitor treatment.

lated state, 4E-BP interacts strongly with eIF4E, while hyperphosphorylation of 4E-BP leads to detachment from eIF4E, which may subsequently bind to the 5′ cap of mRNAs (30). Following binding to the scaffolding protein eIF4G, eIF4E is phosphorylated at S209 by the kinases Mnk1 and Mnk2. We show here that in macrophage-like THP-1 cells, 4E-BP is constitutively phosphorylated at T37/T46, and treatment with purified Stx1 failed to alter phosphorylation at these residues. Following toxin treatment, we noted the rapid (within 1 h) but transient phosphorylation of 4E-BP at S65. Our data are in accordance with the findings of Colpoys et al. (9) showing that treatment of the intestinal epithelial cell line Hct-8 with Stx1 resulted in increased 4E-BP phosphorylation at S65. Toxin-mediated increases in phosphorylation at S65 may reduce the affinity of 4E-BP for eIF4E, since we have shown a lack of hyperphosphorylated 4E-BP associated with phospho-eIF4E/m⁷GTP-Sepharose 4B complexes. MAPK and Mnk1 activation, eIF4E phosphorylation, and cytokine expression by Stx1-treated THP-1 cells require toxin enzymatic activity; treatment of cells with purified Stx1A⁻ or Stx1 B subunits did not trigger these responses (5, 20). In contrast, Stx1A⁻ triggered 4E-BP hyperphosphorylation, although to a lesser extent than Stx1,

suggesting that signaling pathways involved in this response may not require delivery of functional Stxs to the ER. Whether the highly transient nature of 4E-BP activation by Stx1 limits cytokine expression will require additional experiments.

We have shown that Stx1-mediated 4E-BP hyperphosphorylation occurs through the PI3K/Akt/mTOR pathway. PI3K is a membrane-associated lipid-modifying enzyme containing a regulatory subunit (p85) and a catalytic subunit (p110). Following phosphorylation of p85 tyrosine residues, activated PI3K phosphorylates the D3 position of the inositol ring in plasma membrane lipids to generate phospholipid second messengers, further leading to release of Ca^{2+} ions from the ER. Changes in membrane phospholipids localize kinases containing pleckstrin homology domains to the membrane, including PDK1 and Akt (4, 43). PDK1 and mTOR activate Akt by phosphorylation at positions T308 and S473, respectively (21, 40). We have shown that Stx1 activated PI3K, which may lead to generation of phospholipid second messengers, release of Ca^{2+} from intracellular stores, and activation of Akt in macrophage-like THP-1 cells. In accordance with the data showing that optimal 4E-BP hyperphosphorylation requires toxin enzymatic activity, Stx1A⁻ and B subunits only partially activated
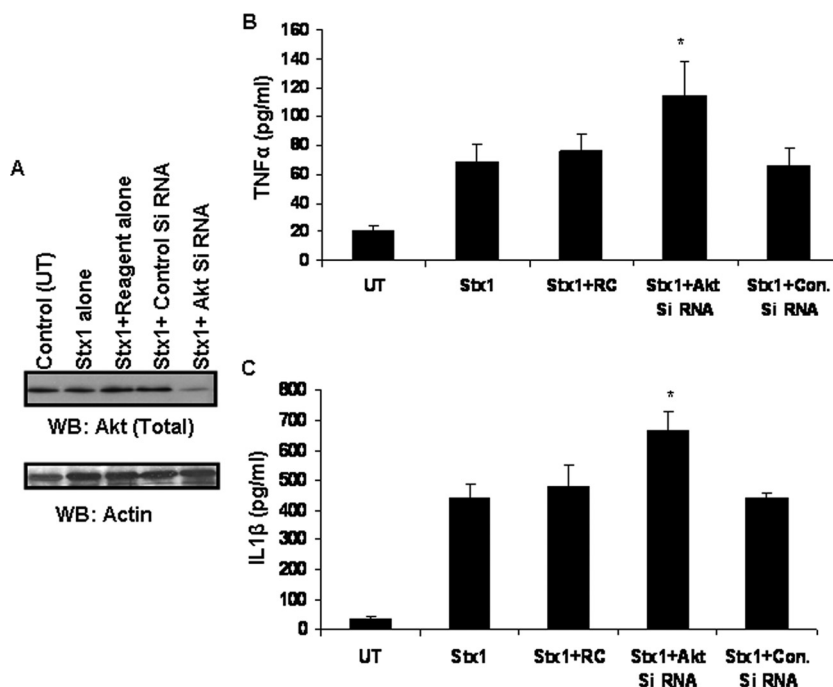
FIG. 9. Effect of Akt knockdown on Stx1-induced production of soluble cytokines. Differentiated THP-1 cells were transfected with Akt-specific siRNA or a nonspecific siRNA control for 48 h. Cells were stimulated with Stx1 for 24 h. (A) Cell lysates were prepared and Western blotting (WB) performed using total Akt antibody. Blots were stripped and reprobed with antibody recognizing actin for equal protein loading. Control (UT), untransfected cells; Control siRNA, nonspecific siRNA. (B and C) Cell supernatants were collected, and soluble TNF-α and IL-1β were quantified by ELISA. All values are expressed in pg/ml ± SEM. Asterisks (∗) represent significant differences ($P < 0.05$) between results with Stx1 alone versus those with Stx1 plus Akt siRNA transfection. RC, reagent control; Con. Si RNA, nonspecific siRNA.

PI3K. Signaling through the PI3K pathway alone, however, is not sufficient for cytokine production; neither Stx1A⁻ nor B subunits will elicit TNF-α or IL-1β expression from THP-1 cells. Cytokine expression appears to require the retrograde transport of functional toxin to the ER, activation of signaling pathways, and the phosphorylation of eIF4E (5, 27).

Consistent with PI3K activation, we noted increased cytosolic Ca^{2+} levels in Stx1- and Stx1A⁻-treated cells. Recently we showed that Stx1 activates the ER stress response in undifferentiated THP-1 cells via a mechanism requiring the retrograde translocation of functional toxin to the ER (27). Stx1 activation of ER stress also triggered the release of Ca^{2+} from ER stores. Collectively, these data suggest that Stxs may alter normal Ca^{2+} homeostasis via multiple mechanisms. Alterations in intracellular Ca^{2+} stores may lead to the activation of a broad array of signaling cascades (6). The role of Stx1-mediated changes in Ca^{2+} localization and regulation of cytokine expression will require further studies.

The precise role of the PI3K/Akt/mTOR pathway in regulation of cytokine expression has not been fully characterized. Thomas et al. (48) reported that respiratory syncytial virus infection of airway epithelial cells resulted in PI3K, Akt, and GSK-3 activation, leading to NF-κB-mediated induction of cytokine gene expression. Inhibition of PI3K activation resulted in rapid apoptotic cell death and blocked respiratory syncytial virus-induced NF-κB activation. Reddy et al. (36) showed that TNF-α induced PI3K and Akt activation in the human myeloid cell line U937, and PI3K activation was essential for increased expression of an NF-κB-dependent reporter

gene. Based on these earlier studies and our demonstration of a positive role for Stx1-induced eIF4E activation in cytokine expression, we predicted that 4E-BP hyperphosphorylation would be associated with increased eIF4E release and increased cytokine production. We found, however, that 4E-BP activation is short-lived, correlating with the transient increase in total protein synthesis we previously noted in toxin-treated THP-1 cells (12). Transfection of THP-1 cells with Akt-specific siRNA and inhibitors of PI3K, Akt, and mTOR all increased cytokine production 24 h after Stx1 treatment. Moreover, the kinase inhibitors alone modestly increased TNF-α and IL-1β production. Thus, our findings are in accordance with those of earlier studies showing that inhibition of the PI3K/Akt pathway increased cytokine and tissue factor expression induced by LPS treatment of murine and human macrophages (18, 26, 29), and activation of the PI3K/Akt pathway by insulin reduced inflammation in mice administered LPS (24). A number of mechanisms may be contributing to PI3K/Akt-mediated negative regulation of cytokine expression. For example, it is known that LPS triggering of the PI3K/Akt pathway reduced MAPK and NF-κB activities through the activation of the negative regulators Raf-1 and IκB kinase and inactivation of the positive regulator GSK-3α/β, leading to reduced activation of transcription factors involved in cytokine gene expression (18). Recently Martin et al. (31) showed that GSK-3α/β is a key regulator in determining the relative expression of pro- and anti-inflammatory mediators by human peripheral blood monocytes. Following GSK-3α/β inhibition, Toll-like receptor 2 (TLR2), TLR4, TLR5, and TLR9 agonists induced IL-10

production while suppressing production of the proinflammatory cytokines IL-1β, IL-6, IL-12p40, and gamma interferon. Akt-dependent phosphorylation of GSK-3α/β is associated with the abrogation of positive signaling for cytokine expression, and we have shown that Akt activated by Stx1 is functional in that GSK-3α/β is phosphorylated. Thus, Stx-mediated PI3K/Akt/mTOR activation may have a brief positive effect leading to 4E-BP hyperphosphorylation but may ultimately have a negative influence on cytokine expression due to increased phosphorylation and inactivation of GSK-3α/β.

ACKNOWLEDGMENTS

REFERENCES

1. **Asnaghi, L., P. Bruno, M. Priulla, and A. Nicolin.** 2004. mTOR: a protein kinase switching between life and death. Pharmacol. Res. **50:**545–549.
2. **Berridge, M. J.** 1993. Inositol trisphosphate and calcium signalling. Nature **361:**315–325.
3. **Cameron, P., S. J. Smith, M. A. Giembycz, D. Rotondo, and R. Plevin.** 2003. Verotoxin activates mitogen-activated protein kinase in human peripheral blood monocytes: role in apoptosis and proinflammatory cytokine release. Br. J. Pharmacol. **140:**1320–1330.
4. **Cantley, L. C.** 2002. The phosphoinositide 3-kinase pathway. Science **296:**1655–1657.
5. **Cherla, R. P., S.-Y. Lee, P. L. Mees, and V. L. Tesh.** 2006. Shiga toxin 1-induced cytokine production is mediated by MAP kinase pathways and translation initiation factor eIF4E in the macrophage-like THP-1 cell line. J. Leukoc. Biol. **79:**397–407.
6. **Clapham, D. E.** 2007. Calcium signaling. Cell **131:**1047–1058.
7. **Coller, J., and R. Parker.** 2004. Eukaryotic mRNA decapping. Annu. Rev. Biochem. **73:**861–890.
8. **Coller, J., and R. Parker.** 2005. General translational repression by activators of mRNA decapping. Cell **122:**875–886.
9. **Colpoys, W. E., B. H. Cochran, T. M. Carducci, and C. M. Thorpe.** 2004. Shiga toxins activate translational regulation pathways in intestinal epithelial cells. Cell. Signal. **17:**891–899.
10. **Cross, D. A., D. R. Alessi, P. Cohen, M. Andjelkovich, and B. A. Hemmings.** 1995. Inhibition of glycogen synthase kinase-3 by insulin mediated by protein kinase B. Nature **378:**785–789.
11. **Endo, Y., K. Tsurugi, T. Yutsudo, Y. Takeda, Y. Ogasawara, and K. Igarashi.** 1988. Site of action of a Vero toxin (VT2) from *Escherichia coli* O157:H7 and of Shiga toxin on eukaryotic ribosomes. RNA *N*-glycosidase activity of the toxins. Eur. J. Biochem. **171:**45–50.
12. **Foster, G. H., C. S. Armstrong, R. Sakiri, and V. L. Tesh.** 2000. Shiga toxin-induced tumor necrosis factor alpha expression: requirement for toxin enzymatic activity and monocyte protein kinase C and protein tyrosine kinases. Infect. Immun. **68:**5183–5189.
13. **Franke, T. F., D. R. Kaplan, L. C. Cantley, and A. Toker.** 1997. Direct regulation of the Akt proto-oncogene product by phosphatidylinositol-3,4-bisphosphate. Science **275:**665–668.
14. **Garneau, N. L., J. Wilusz, and C. J. Wilusz.** 2007. The highways and byways of mRNA decay. Nat. Rev. Mol. Cell Biol. **8:**113–126.
15. **Gingras, A.-C., S. G. Kennedy, M. A. O'Leary, N. Sonenberg, and N. Hay.** 1998. 4E-BP1, a repressor of mRNA translation, is phosphorylated and inactivated by the Akt (PKB) signaling pathway. Genes Dev. **12:**502–513.
16. **Gingras, A.-C., B. Raught, S. P. Gygi, A. Niedzwiecka, M. Miron, S. K. Burley, R. D. Polakiewicz, A. Wyslouch-Cieszynska, R. Aebersold, and N. Sonenberg.** 2001. Hierarchical phosphorylation of the translation inhibitor 4E-BP1. Genes Dev. **15:**2852–2864.
17. **Gingras, A.-C., B. Raught, and N. Sonenberg.** 1999. eIF4 initiation factors: effectors of mRNA recruitment to ribosomes and regulators of translation. Annu. Rev. Biochem. **68:**913–963.
18. **Guha, M., and N. Mackman.** 2002. The phosphatidylinositol 3-kinase-Akt pathway limits lipopolysaccharide activation of signaling pathways and expression of inflammatory mediators in human monocytic cells. J. Biol. Chem. **277:**32124–32132.
19. **Harrison, L. M., W. van den Hoogen, W. C. E. van Haaften, and V. L. Tesh.** 2005. Chemokine expression in the monocytic cell line THP-1 in response to purified Shiga toxin 1 and/or lipopolysaccharides. Infect. Immun. **73:**403–412.
20. **Harrison, L. M., W. C. E. van Haaften, and V. L. Tesh.** 2004. Regulation of proinflammatory cytokine expression by Shiga toxin 1 and/or lipopolysaccharides in the human monocytic cell line THP-1. Infect. Immun. **72:**2618–2627.
21. **Hresko, R. C., and M. Mueckler.** 2005. mTOR-RICTOR is the Ser⁴⁷³ kinase for Akt/protein kinase B in 3T3-L1 adipocytes. J. Biol. Chem. **280:**40406–40416.
22. **Kabbara, A. A., and D. G. Allen.** 2001. The use of the indicator fluo-5N to measure sarcoplasmic reticulum calcium in single muscle fibers of the cane toad. J. Physiol. **534:**87–97.
23. **Keepers, T. R., L. K. Gross, and T. G. Obrig.** 2007. Monocyte chemoattractant protein 1, macrophage inflammatory protein 1α, and RANTES recruit macrophages to the kidney in a mouse model of hemolytic-uremic syndrome. Infect. Immun. **75:**1229–1236.
24. **Kidd, L. B., G. A. Schabbauer, J. P. Luyendyk, T. D. Holscher, R. E. Tilley, M. Tencati, and N. Mackman.** 2008. Insulin activation of the phosphatidylinositol 3-kinase/protein kinase B (Akt) pathway reduces lipopolysaccharide-induced inflammation in mice. J. Pharmacol. Exp. Ther. **326:**348–353.
25. **Kyriakis, J. M., and J. Avruch.** 1996. Sounding the alarm: protein kinase cascades activated by stress and inflammation. J. Biol. Chem. **271:**24313–24316.
26. **Lee, J. S., W. M. Nauseef, A. Moeenrezakhanlou, L. M. Sly, S. Noubir, K. G. Leidal, J. M. Schlomann, G. Krystal, and N. E. Reiner.** 2007. Monocyte p110alpha phosphatidylinositol 3-kinase regulates phagocytosis, the phagocyte oxidase, and cytokine production. J. Leukoc. Biol. **81:**1548–1561.
27. **Lee, S.-Y., M.-S. Lee, R. P. Cherla, and V. L. Tesh.** 2008. Shiga toxin 1 induces apoptosis through the endoplasmic reticulum stress response in human monocytic cells. Cell. Microbiol. **10:**770–780.
28. **Lingwood, C. A.** 2003. Shiga toxin receptor glycolipid binding. Pathology and utility. Methods Mol. Med. **73:**165–186.
29. **Luyendyk, J. P., G. A. Schabbauer, M. Tencati, T. Holscher, R. Pawlinski, and N. Mackman.** 2008. Genetic analysis of the role of the PI3K-Akt pathway in lipopolysaccharide-induced cytokine and tissue factor gene expression in monocytes/macrophages. J. Immunol. **180:**4218–4226.
30. **Mamane, Y., E. Petroulakis, L. Rong, K. Yoshida, L. W. Ler, and N. Sonenberg.** 2004. eIF4E—from translation to transformation. Oncogene **23:**3172–3179.
31. **Martin, M., K. Rehani, R. S. Jope, and S. M. Michalek.** 2005. Toll-like receptor-mediated cytokine production is differentially regulated by glycogen synthase kinase 3. Nat. Immunol. **6:**777–784.
32. **Ohmura, M., S. Yamasaki, H. Kurazono, K. Kashiwagi, K. Igarashi, and Y. Takeda.** 1993. Characterization of non-toxic mutant toxins of Vero toxin 1 that were constructed by replacing amino acids in the A subunit. Microb. Pathog. **15:**169–176.
33. **Park, M. K., O. H. Petersen, and A. V. Tepikin.** 2000. The endoplasmic reticulum as one continuous Ca²⁺ pool: visualization of rapid Ca²⁺ movements and equilibration. EMBO J. **19:**5729–5739.
34. **Ramegowda, B., and V. L. Tesh.** 1996. Differentiation-associated toxin receptor modulation, cytokine production and sensitivity to Shiga-like toxins in human monocytes and monocytic cell lines. Infect. Immun. **64:**1173–1180.
35. **Ramegowda, B., J. E. Samuel, and V. L. Tesh.** 1999. Interaction of Shiga toxins with human brain microvascular endothelial cells: cytokines as sensitizing agents. J. Infect. Dis. **180:**1205–1213.
36. **Reddy, S. A. G., J. H. Huang, and W. S.-L. Liao.** 2000. Phosphatidylinositol 3-kinase as a mediator of TNF-induced activation of NF-κB. J. Immunol. **164:**1355–1363.
37. **Richter, J. D., and N. Sonenberg.** 2005. Regulation of cap-dependent translation by eIF4E inhibitory proteins. Nature **433:**477–480.
38. **Sakiri, R., B. Ramegowda, and V. L. Tesh.** 1998. Shiga toxin type 1 activates tumor necrosis factor-α gene transcription and nuclear translocation of the transcriptional activators nuclear factor-κB and activator protein-1. Blood **92:**558–566.
39. **Sandvig, K., and B. van Deurs.** 2002. Transport of protein toxins into cells: pathways used by ricin, cholera toxin and Shiga toxin. FEBS Lett. **529:**49–53.
40. **Sarbassov, D. D., D. A. Guertin, S. M. Ali, and D. M. Sabatini.** 2005. Phosphorylation and regulation of Akt/PKB by the rictor-mTOR complex. Science **307:**1098–1101.
41. **Saxena, S. K., A. D. O'Brien, and E. J. Ackerman.** 1989. Shiga toxin, Shiga-like toxin II variant, and ricin are all single-site RNA *N*-glycosidases of 28S RNA when microinjected into *Xenopus* oocytes. J. Biol. Chem. **264:**596–601.
42. **Schaeffer, H. J., and M. J. Weber.** 1999. Mitogen-activated protein kinases: specific messages from ubiquitous messengers. Mol. Cell. Biol. **19:**2435–2444.
43. **Shaw, R. J., and L. C. Cantley.** 2006. Ras, PI(3)K and mTOR signalling controls tumour cell growth. Nature **441:**424–430.
44. **Stricklett, P. K., A. K. Hughes, Z. Ergonul, and D. E. Kohan.** 2002. Molecular basis for up-regulation by inflammatory cytokines of Shiga toxin 1 cytotoxicity and globotriaosylceramide expression. J. Infect. Dis. **186:**976–982.
45. **Tarr, P. I., C. A. Gordon, and W. I. Chandler.** 2005. Shiga toxin-producing *Escherichia coli* and haemolytic uraemic syndrome. Lancet **365:**1073–1086.
46. **Taylor, F. B., Jr., V. L. Tesh, L. DeBault, A. Li, A. C. K. Chang, S. D. Kosanke, T. J. Pysher, and R. L. Siegler.** 1999. Characterization of the baboon responses to Shiga-like toxin: descriptive study of a new primate model of toxic responses to Stx-1. Am. J. Pathol. **154:**1285–1299.
47. **Tesh, V. L., J. A. Burris, J. W. Owens, V. M. Gordon, E. A. Wadolkowski,**

A. D. O'Brien, and J. E. Samuel. 1993. Comparison of the relative toxicities of Shiga-like toxins type I and type II for mice. Infect. Immun. **61:**3392–3402.

48. **Thomas, K. W., M. M. Monack, J. M. Stabler, T. Yarovinsky, A. B. Carter, and G. W. Hunninghake.** 2002. Respiratory syncytial virus inhibits apoptosis and induces NF-κB activity through a phosphatidylinositol 3-kinase-dependent pathway. J. Biol. Chem. **277:**492–501.

49. **Thorpe, C. M., W. E. Smith, B. P. Hurley, and D. W. K. Acheson.** 2001. Shiga toxins induce, superinduce, and stabilize a variety of C-X-C chemokine mRNAs in intestinal epithelial cells, resulting in increased chemokine expression. Infect. Immun. **69:**6140–6147.

50. **van de Kar, N. C. A. J., L. A. H. Monnens, M. A. Karmali, and V. W. M. van Hinsbergh.** 1992. Tumor necrosis factor and interleukin 1 induce expression of the verocytotoxin receptor globotriaosylceramide on human endothelial cells: implications for the pathogenesis of the hemolytic uremic syndrome. Blood **80:**2755–2764.

51. **van Setten, P. A., L. A. H. Monnens, R. G. G. Verstraten, L. P. W. J. van den Heuvel, and V. W. M. van Hinsbergh.** 1996. Effects of verocytotoxin-1 on nonadherent monocytes: binding characteristics, protein synthesis inhibition, and induction of cytokine release. Blood **88:**174–183.

52. **von Manteuffel, S. R., A.-C. Gingras, X. F. Ming, N. Sonenberg, and G. Thomas.** 1996. 4E-BP1 phosphorylation is mediated by the FRAP-p70s6k pathway and is independent of mitogen-activated protein kinase. Proc. Natl. Acad. Sci. USA **93:**4076–4080.

53. **Zoja, C., S. Angioletti, R. Donadelli, C. Zanchi, S. Tomasoni, E. Binda, B. Imberti, M. te Loo, L. Monnens, G. Remuzzi, and M. Morigi.** 2002. Shiga toxin-2 triggers endothelial leukocyte adhesion and transmigration via NF-κB dependent up-regulation of IL-8 and MCP-1. Kidney Int. **62:**846–856.

Editor: S. R. Blanke